

# Thermal Control System for Electrical Components of Hybrid-Electric Powered Low Carbon Air Vehicle

1<sup>st</sup> Mingxing Yu

*Research Institute of Aero-  
Engine  
Beihang University  
Beijing, China  
yumingxing1314@buaa.edu.cn*

2<sup>nd</sup> Zhi Tao

*Research Institute of Aero-  
Engine  
Beihang University  
Beijing, China  
19820912@sina.com*

3<sup>rd</sup> Haiwang Li

*Research Institute of Aero-  
Engine  
Beihang University  
Beijing, China  
lihaiwang@buaa.edu.cn*

4<sup>th</sup> Gang Xie

*Flying College of Beihang  
University  
Beihang University  
Beijing, China  
xiegang@buaa.edu.cn*

**Abstract**—This paper presents the design and analysis of thermal control systems (TCS) for electrical components of hybrid-electric low carbon air vehicles, addressing the TCS challenges set by the ICAO's 2050 net-zero carbon emissions goal. We explore various heat sinks and TCS architectures through theoretical modeling and simulation using Flomaster and MATLAB/Simulink, focusing on heat sink effectiveness and system integration. Two distinct TCS architectures, centralized and distributed, are analyzed for their performance in managing thermal loads of electrical components across different flight phases. Our findings highlight the superior efficiency of the distributed system in maintaining component temperatures within safe operational limits, thereby enhancing aircraft sustainability and operational safety.

**Keywords**—thermal control system, electrical components, hybrid-electric powered, low carbon vehicle

## I. INTRODUCTION

In October 2022, the International Civil Aviation Organization (ICAO) set a transformative climate goal for the aviation industry, aiming to achieve net zero carbon emissions in international aviation operations by 2050. This objective highlights the pressing need for innovative advancements in aviation power, especially considering that approximately 79% of aviation emissions originate from the combustion of aviation kerosene. As the sector moves towards green and sustainable development, hybrid-electric powered low carbon air vehicle emerges as a key technological direction. However, this transition introduces significant engineering challenges, particularly in the development of Thermal control Systems (TCS). Essential for maintaining the operational safety and efficiency of hybrid-electric aircraft, TCS manage the substantial waste heat generated by electrical components and ensure them remain within appropriate operating temperatures. However, TCS for hybrid-electric aircraft face numerous challenges, particularly in terms of architecture design and performance analysis. Consequently, these areas have become hotspots in current research, which have attracted the attention of many researchers.

Emphasis has been placed on the pressing technical challenges that TCS must address in the literature, particularly the need for lightweight and efficient cooling mechanisms in hybrid-electric aircraft. References [1,2] proposed innovative solutions like thermoacoustic refrigeration systems, leveraging waste heat from turbofan engines for cooling, presenting an

alternative to conventional electric-powered systems. Reference [3] provided a comprehensive analysis of potential TCS technologies, considering their integration, safety, and operational impacts. Reference [4] outlined thermal requirements for specific aircraft designs, underlining the importance of adhering to established standards and guidelines. Reference [5] critically reviewed existing solutions and suggested that the integration of nanofluids and skin heat exchangers may offer promising avenues for future research and development.

The design and optimization of TCS have been explored through various studies proposing novel system architectures and methodologies. Reference [6,7] investigated TCS designs for different electric aircraft propulsion concepts, emphasizing the impact of requirement changes on TCS subcomponents. Reference [8] presented a framework for simulating and optimizing TCS at a system level, focusing on minimizing weight gain and power utilization. Reference [9] introduced a graph-based tool for generating and evaluating TCS architecture concepts, applicable to a range of aircraft platforms. Reference [10] investigated ram air-based TCS, providing a model to estimate the impacts of mass, drag, and fuel burn. Reference [11] discussed weight sensitivity in TCS components, highlighting the trade-offs between thermal performance and system weight. Reference [12] discussed the need for advancements in electrical component efficiencies and cooling technology to achieve acceptable weight penalties for TCS.

Understanding the trade-offs analysis in TCS design is crucial for optimizing aircraft performance. Reference [13] analyzed the cooling abilities and performance penalties of various heat sinks under different flight conditions, providing insights into the best configurations for thermal control. Reference [14] explored the relationship between exergy destruction minimization and conventional design metrics, offering a novel approach to assessing TCS performance. Case studies provided in References [15-17] detailed the integration of TCS into specific aircraft designs. These studies demonstrated the practical application of TCS technologies and the challenges of integrating them into existing aircraft concepts, such as the ECO-150 regional airliner and commercial single-aisle aircraft with hybrid electric propulsion systems.

Building on the comprehensive review of existing thermal control technological advances and development challenges, this study aims to advance the architecture design and performance analysis of thermal control systems for hybrid-electric powered low carbon air vehicle. We address the critical need for lightweight, efficient, and integrated cooling solutions that are capable of operating across diverse flight conditions. The forthcoming sections will detail our methodological approach, which leverages advanced simulation tools to rigorously test and refine TCS architectures. This is followed by the presentation of our results, where the performance of proposed systems under simulated flight conditions is thoroughly evaluated.

## II. METHODS

In this section, the hybrid-electric propulsion architecture with its operating principles and thermal requirements are firstly outlined. Then the integration of theoretical modelling and simulation is used to evaluate multiple heat sinks and their cooling capability during overall flight phases. Two TCS architectures are then proposed to meet the stringent thermal requirements of electrical components and their performances are simulated by using Matlab/Simulink models.

### A. Hybrid-electric propulsion architecture and thermal requirements

The schematic diagram of hybrid-electric propulsion for low carbon air vehicle and its thermal control system is

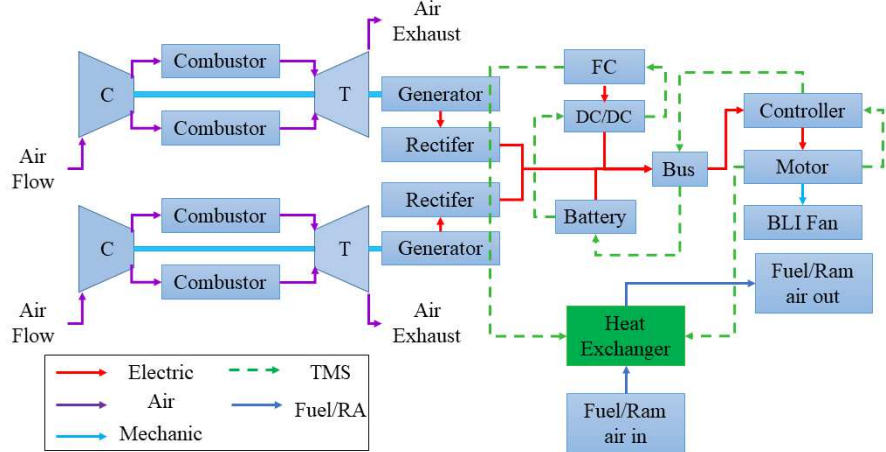


Fig. 1. Schematic diagram of hybrid-electric propulsion for low carbon air vehicle and its thermal control system.

Fig.2 illustrates the changes in flight speed (Mach number) and altitude of the reference aircraft over a 120-minute period. Within the first 20 minutes after takeoff, the aircraft rapidly ascends to approximately 0.75 Mach and an altitude of 35,000 feet, maintaining these conditions until the 100-minute mark. Subsequently, over the next 20 minutes, the aircraft quickly decelerates and descends back to ground level.

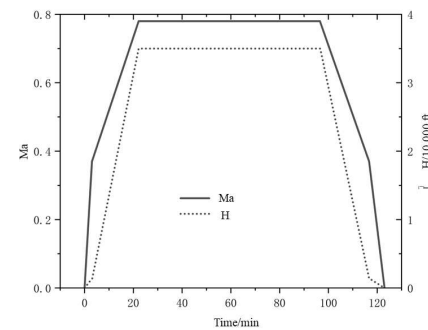


Fig. 2. Flight speed and altitude of the reference aircraft.

In the depicted phases of the aircraft's flight—taxi out, take off, climb, cruise, descent, landing, and taxi in—the operational status and thermal load of the electrical equipment are presented, as shown in TABLE I. During the taxi out and taxi in phases, the propulsion motors are powered exclusively by batteries. In the Take off phase, both batteries and motors jointly supply the necessary electrical power. During the climb

phase, additional energy from the generator supplements the power supply. In the cruise phase, which is the longest duration of the flight, both batteries and the generator drive the motors. During the descent and landing phases, the generator primarily powers the motors, while surplus electrical energy is directed towards recharging the batteries, thus facilitating energy recovery and utilization.

TABLE I. OPERATIONAL DYNAMICS AND THERMAL LOAD OF AIRCRAFT ELECTRICAL COMPONENTS ACROSS FLIGHT PHASES.

Phases	Taxi out	Take off	Climb	Cruise	Descent	Landing	Taxi in
Duration	9min	2min	19.7min	74.1min	20min	6min	5min
Components in Operation	Battery+Motor +Controller+D C/DC	Battery +FC+ Motor+Control ler +DC/DC	Generator+ Battery +FC+ Motor+Control ler + Rectifier +DC/DC	Generator+ Battery + Motor+Control ler + Rectifier +DC/DC	Generator+ Battery + rectifier +DC/DC	Generator+ Battery + rectifier +DC/DC	Battery+Motor +Controller+D C/DC
Thermal Load	54.45kW	224.45kW	320.45kW	150.93kW	101.45kW	101.45kW	54.45kW

The coolant requirements and operational temperature limits for electrical components of the aircraft, organized into three main systems: power generation, energy storage, and propulsion are described in TABLE II. For the power generation system, the components listed are two generators and two rectifiers, utilizing Jet Oil II and PGW40% as coolants, respectively. The minimum coolant flow rates are set at 45L/min and 80L/min, while the maximum permissible temperatures are 45°C and 70°C, respectively. In the energy storage system, the battery and fuel cell (FC), both cooled with PGW40%, require coolant flow rates of 20L/min and 100L/min, with temperature ceilings of 20°C and 60°C, respectively. Lastly, the propulsion system comprises a motor and its controller, both utilizing Jet Oil II, with required coolant flows of 60L/min and 80L/min and temperature limits of 60°C and 70°C.

generation rates depending on flight phase necessitates a dynamically adaptable thermal control system that can handle the shifting thermal loads efficiently. Thus, while heat sinks are a pivotal component of the aircraft's thermal control strategy, their design and integration require careful consideration to balance effectiveness with the practical limitations of aircraft operations.

In response to these complexities, a systematic assessment of various thermal control heat sinks becomes imperative and simulation models have been established in simulation tool Flomaster. Four primary options are assessed: a collector fuel tank heat sink, an in-wing fuel tank recirculatory heat sink, a ram air heat sink, and an engine fan air heat sink.

The maximum heat removal rate by fuel and air is calculated through two distinct mechanisms, described by Equation (1) and Equation (2).

$$q_f = -\dot{m}_f c_{p,f} (T_{f,lim} - T_f) \quad (1)$$

$$q_a = \max(\dot{m}_a c_{p,a} \eta_{aHEX} (T_{load,max} - T_{ex,a}), 0) \quad (2)$$

Where  $q_f$  and  $q_a$  represent the cooling capabilities of fuel and ram air, respectively.  $\dot{m}_f$ ,  $c_{p,f}$  is the mass flow rate of the fuel and its specific heat capacity, respectively, and the fuel should not exceed the threshold temperature ( $T_{f,lim}$ ) to prevent coking, and  $T_f$  represents the actual temperature of the fuel. Equation (2) represents the maximum heat removal rate by air heat exchanger (aHEX). It incorporates the mass flow rate of ram air( $\dot{m}_a$ ), the specific heat capacity of air( $c_{p,a}$ ), the efficiency of the heat exchanger( $\eta_{aHEX}$ ), the maximum allowable temperature of the electrical component system ( $T_{load,max}$ ) and the external temperature of the air ( $T_{ex,a}$ ).

#### a) Single heat sink methods

Collector fuel tank heat sink. The principle of the collector fuel tank heat sink scheme is that the fuel from the wing tank/central wing tank flows into the collector tank, where the fuel in the collector tank passes through a heat exchanger before being supplied to the engine, dissipating heat for the thermal control system to fuel. Under a 330-minute flight phases in hot weather conditions, the cooling capacity is calculated as shown in Fig.3. The instantaneous heat exchange power extracted by adopting the collector tank heat sink

TABLE II. COOLANT REQUIREMENTS AND TEMPERATURE LIMITS FOR AIRCRAFT ELECTRICAL COMPONENTS.

System	Component	Coolant	M <sub>in,lim</sub>	T <sub>in,lim</sub>
Power Generation	Generator × 2	Jet Oil II	≤45L/min	≥45°C
	Rectifier × 2	PGW40%	≤80L/min	≥70°C
Energy Storage	Battery	PGW40%	≤20L/min	≥20°C
	FC	PGW40%	≤100L/min	≥60°C
Propulsion Motor	Motor	Jet Oil II	≤60L/min	≥60°C
	Controller	Jet Oil II	≤80L/min	≥70°C

#### B. Heat sinks for cooling electrical components

Efficient thermal control systems are essential to maintaining optimal electrical components performance, ensuring safety, and prolonging lifespan. Heat sinks help dissipate the excessive heat generated by both the electrical and mechanical components, which is critical in safeguarding component operation within safe thermal limits.

However, the implementation of heat sinks in hybrid electric aircraft presents several challenges. These include the integration of the heat sink with the aircraft's design without compromising aerodynamic efficiency, managing the added weight, and ensuring that the thermal control system itself does not consume excessive power. Moreover, the variability in heat

scheme can reach a maximum of 84.25 kW and a minimum of 11.36 kW.

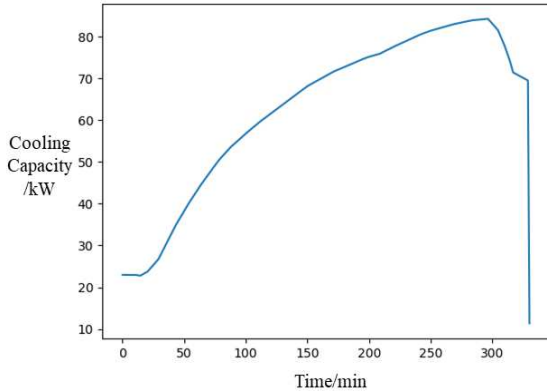


Fig. 3. Cooling capability of collector fuel tank heat sink.

In-wing fuel tank recirculatory heat sink. The in-tank recirculation heat sink method for wing tanks utilizes a dedicated fuel circuit. Fuel is drawn from the wing tank/central wing tank and circulated through a heat exchanger before being returned to its original tank. During this process, the fuel's cold energy is transferred via the heat exchanger to the cooling fluid of the thermal control system, thereby dissipating heat from the thermal load. In a flight phase of 330-minute under hot weather conditions, Fig.4 illustrates the calculated cooling capacity. The range of instantaneous heat exchange power achievable with the wing tank heat sink strategy peaks at 42.37 kW and bottoms out at 39.80 kW.

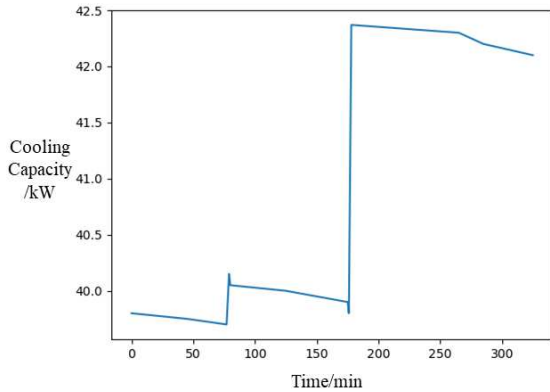


Fig. 4. Cooling capability of in-wing fuel tank recirculatory heat sink.

Ram air heat sink. The methodology employed in the ram air heat sink involves situating the heat exchanger of the thermal control system within the air conditioning system's ram air duct. This configuration facilitates the extraction of cold energy from the ram air, which is then utilized to cool the thermal control system. During a flight scenario spanning 330 minutes in a hot weather setting, the depicted Fig.5 outlines the cooling capabilities. By implementing the ram air heat sink method, the range of heat exchange power that can be achieved fluctuates between a maximum of 146.09 kW and a minimum of 31.32 kW.

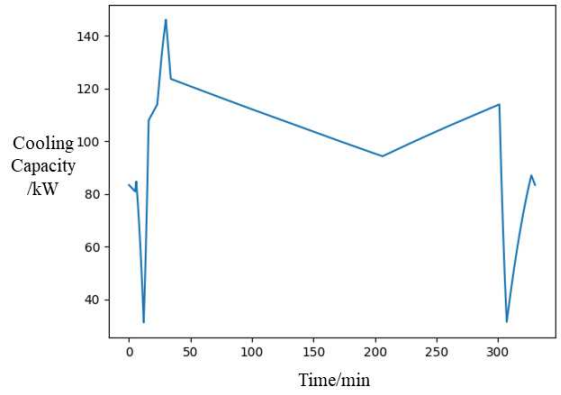


Fig. 5. Cooling capability of ram air heat sink heat sink.

Engine fan air heat sink. This approach entails channeling the airflow from behind the engine fan into the heat exchangers of the thermal control system, where the cold energy harvested from the engine fan air is deployed for managing thermal loads. Observations taken 12 minutes prior and 301 minutes subsequent to operation indicate that the air temperature exceeding 70°C renders it unsuitable as a definitive heat sink. In terms of cooling capacity over a 330-minute flight duration in high-temperature conditions, the range of instantaneous heat exchange power possible with the use of the engine fan air heat sink method spans from a minimum of 4.82 kW to a maximum of 66.25 kW, as shown in Fig.6.

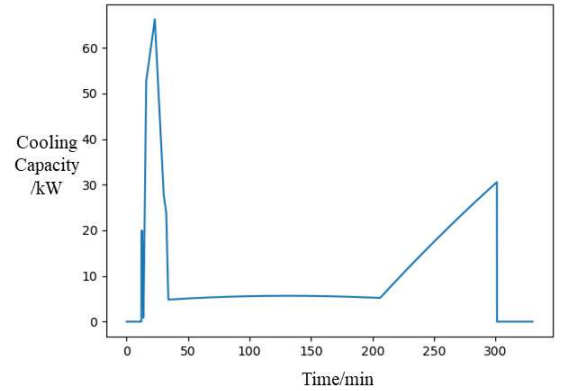


Fig. 6. Cooling capability of engine fan air heat sink.

### b) Combined heat sinks methods

The analysis from Section 2.2.1 demonstrates that no single heat sink can provide the cooling capacity required by the electrical components throughout the entire flight phase. Therefore, several composite heat sink designs are proposed, which include combinations such as 1) collector fuel tank with ram air, 2) in-wing fuel tank recirculation with ram air, 3) collector fuel tank with in-wing fuel tank recirculation and ram air, and 4) a comprehensive combination of all three mentioned systems.

Combined option 1 employs a combined heat sink mode using the collector tank and ram air. The fuel in the collector tank exchanges heat with the liquid coolant PGW through an oil-liquid heat exchanger. Ram air exchanges heat with PGW

through an air-liquid heat exchanger. Under hot weather conditions and a 330-minute flight envelope, the instantaneous heat exchange power can reach a maximum of 197.35 kW at 296.4 minutes into the flight, and a minimum of 54.21 kW at 12 minutes, as illustrated in Fig.7.

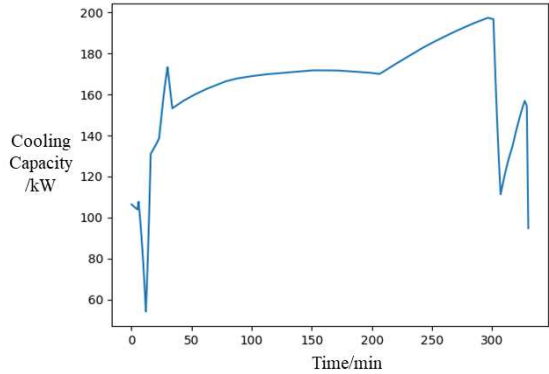


Fig. 7. Cooling capability of combined option 1.

Combined option 2 utilizes a combination heat sink mode involving in-wing fuel tank recirculation and ram air. The fuel within the wing tank circulates through an oil-liquid heat exchanger to exchange heat with the liquid coolant PGW. Similarly, ram air is heated through an air-liquid heat exchanger with PGW. As depicted in Fig.8, in the 330-minute flight envelope under hot weather conditions, the maximum instantaneous heat exchange power is 185.94 kW, occurring at 30 minutes, with a minimum of 71.14 kW at 307 minutes.

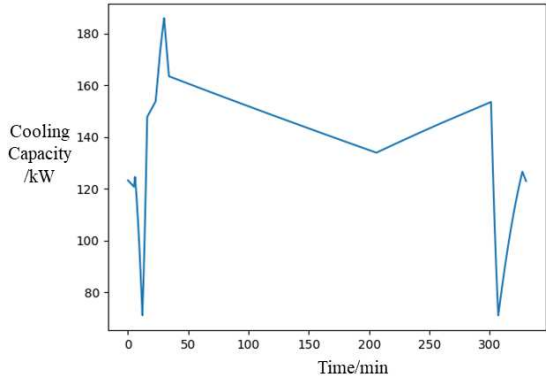


Fig. 8. Cooling capability of combined option 2.

Combined option 3 combines the collector tank, in-wing fuel tank recirculation, and ram air for its heat sink mode. Both the collector and wing tank fuels exchange heat with the liquid coolant PGW through the oil-liquid heat exchanger. Ram air is also heated through the air-liquid heat exchanger with PGW. During a 330-minute flight under hot conditions, the combined heat sink scheme can extract a maximum heat exchange power of 236.95 kW at 296.4 minutes and a minimum of 94 kW at 12 minutes, as shown in Fig.9.

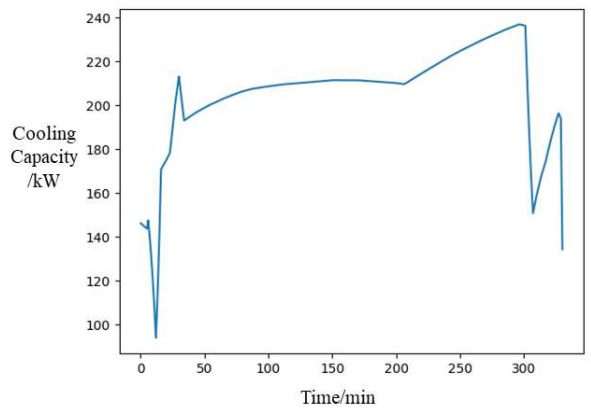


Fig. 9. Cooling capability of combined option 3.

Combined option 4 incorporates the collector tank, in-wing fuel tank recirculation, ram air, and engine fan air into its heat sink mode. The fuels from both the collector and wing tanks are heated through an oil-liquid heat exchanger with PGW, while ram air and engine fan air are heated through an air-liquid heat exchanger with PGW. As illustrated in Fig.10, under hot weather conditions and a 330-minute flight envelope, this combined heat sink extraction scheme can reach a peak heat exchange power of 266.86 kW at 301 minutes and a minimum of 94.08 kW at 12 minutes.

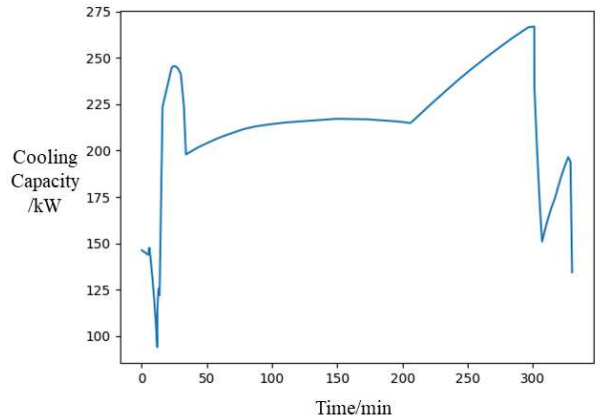


Fig. 10. Cooling capability of combined option 4.

The analysis above indicates that the fuel heat sink is highly compatible with existing thermal control systems and does not induce compensatory losses, making it the primary choice for thermal sinks in hybrid aircraft thermal control systems. However, compared to traditional aircraft, hybrid aircraft have reduced fuel volume, which diminishes the cooling capacity of the fuel heat sink. Additionally, the heat output of thermal control equipment increases, necessitating the introduction of ram air as a new terminal heat sink. The cooling capacity provided by engine fan bleed air throughout all flight phases is less than that of fuel and ram air, and it also impacts engine efficiency while increasing the aircraft's additional aerodynamic drag. Therefore, in the subsequent design of thermal control system architectures, the main considerations are the combinations of the oil tank heat sink, In-wing fuel tank recirculatory heat sink, and ram air heat sink.

As illustrated in Fig. 9, even using these three types of heat sink combinations cannot meet the aircraft's maximum heat dissipation requirements during the climb phase. Hence, during this phase, increasing the inflow of ram air is proposed to adequately supply the heat sink.

### C. TCS architecture design

After the heat sinks are determined, the architecture design of the thermal control system is conducted. Two architectures, centralized thermal control system (CTCS) and distributed thermal control system (DTCS), have been proposed and their performances have been compared by simulation method using MATLAB/Simulink software.

The centralized thermal control architecture with a hybrid coolant loop is presented in Fig.11. Based on the layout of

electrical components, liquid cooling requirements, and heat dissipation power, the thermal control system is designed with two major loops in parallel: the rectifier-battery-generator loop and the DC/DC- motor- controller loop. A fuel cell is integrated in series in the main circuit for cooling, and centralized heat dissipation occurs at heat exchanger with the terminal heat sink (fuel/ram air), with a pump and a reservoir installed in the main circuit to regulate the coolant flow. Two Generators, the motor, and the motor controller utilize oil cooling. Therefore, separate oil cooling circuits are established for these four devices. Heat exchange with the liquid cooling system of the circuit is conducted separately through three oil/coolant heat exchangers, with three pumps respectively adjusting the coolant flow in each oil cooling circuit.

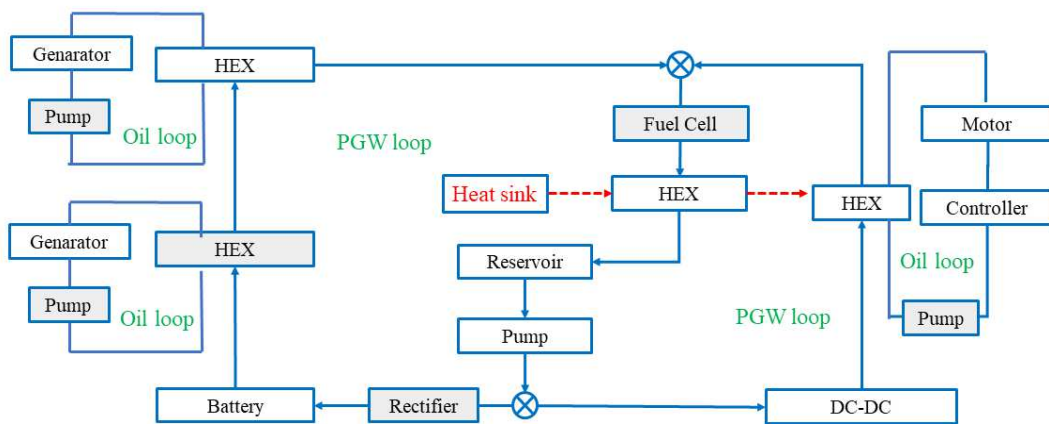


Fig. 11. Architecture of centralized thermal control system.

Fig.12 illustrates the multi-loop distributed thermal control architecture. Based on the layout of the electrical components, liquid cooling requirements, and heat dissipation power, and considering the use of fuel and ram air as heat sinks, the thermal control system is designed as two independent systems. In the fuel heat sink section, three circuits are set up: Two generator circuits and the rectifier-battery circuit, which ultimately conduct heat exchange with the fuel via oil/fuel and liquid coolant/fuel heat exchangers. In the ram air heat sink

section, three circuits are established: motor controller-DC/DC circuit, fuel cell circuit, and motor circuit, ultimately conducting heat exchange with ram air via oil/ram air and liquid coolant/ram air heat exchangers. Pumps, oil tanks and coolant reservoir are installed in each circuit to adjust the coolant flow. Additionally, for circuits with multiple devices, such as the rectifier-battery circuit and the motor controller-DC/DC circuit, three-way valves are installed to individually regulate and control the equipment in the circuit.

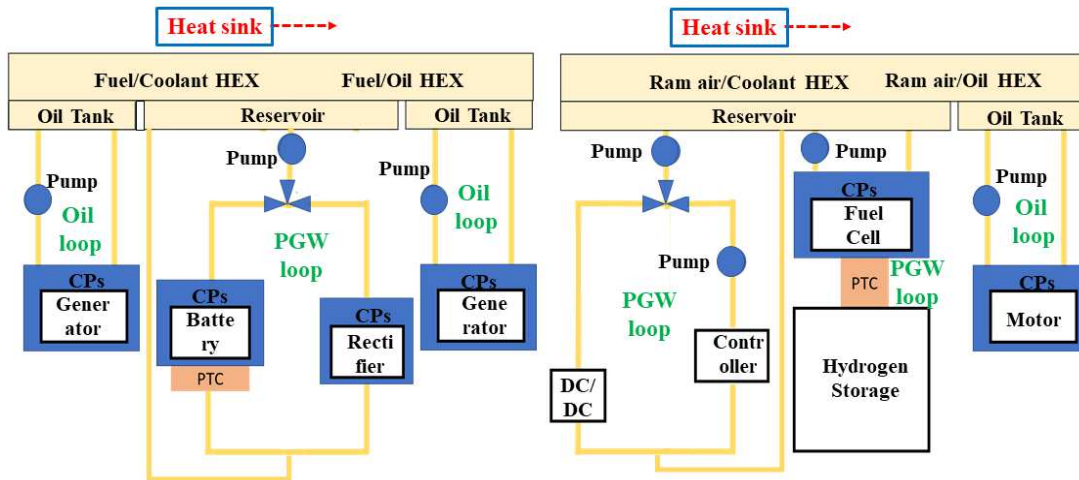


Fig. 12. Architecture of distributed thermal control system.

### III. RESULTS AND CONCLUSIONS

Using MATLAB/Simulink software, models of both CTCS architecture and DTCS architecture were established and simulated. The simulation results of the inlet temperature for the electrical components in CTCS architecture are shown in Fig.13, while the inlet and outlet temperature results for the components in DTCS architecture are shown in Fig.14 and Fig.15.

Fig.13 illustrates the variation of inlet temperatures for different electrical components (Controller, Generator, Motor, Battery, DC/DC Converter, Rectifier, and Fuel Cell) in a CTCS architecture over time, which highlights the different thermal behaviors and cooling requirements of each component in the centralized system. The controller shows a significant increase in outlet temperature, reaching approximately 350 K after 140 seconds. The generator, motor, and battery exhibit moderate temperature rises, stabilizing around 320-330 K. The DC/DC converter, rectifier, and fuel cell show minimal temperature increases, maintaining temperatures just above 300 K throughout the simulation period.

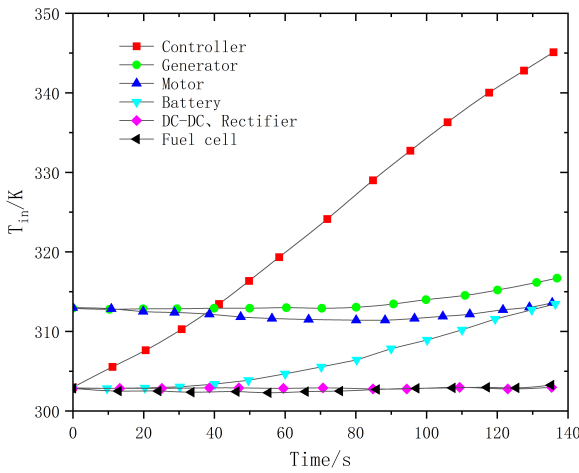


Fig. 13. Inlet temperatures for different electrical components in a CTCS architecture.

Fig.14 depicts the variation in inlet temperatures of electrical components within a DTCS architecture over time. Motor and generator exhibit a gradual increase in temperature, reaching approximately 315 K and 312 K, respectively, by the end of the 140-second period. In contrast, controller, DC/DC converter, and fuel cell maintain a stable inlet temperature of around 305 K. Battery and rectifier show a slight increase, stabilizing at just below 290 K. These results demonstrate the differential thermal load management and the effectiveness of the distributed architecture in maintaining component temperatures within specific ranges.

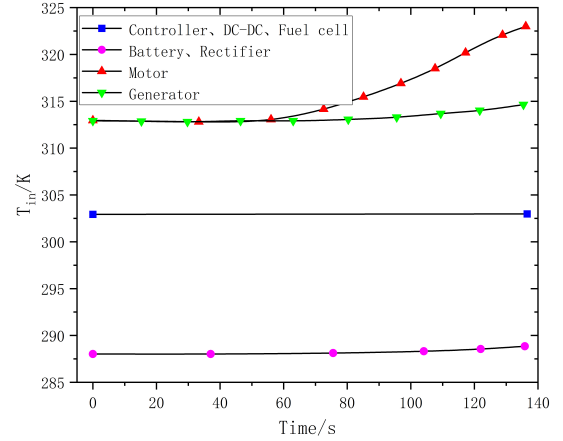


Fig. 14. Inlet temperatures for different electrical components in a DTCS architecture.

Fig.15 presents the temporal evolution of the outlet temperatures for various electrical components in a DTCS architecture. Motor and generator show the highest temperature increases, peaking at around 370 K and 360 K, respectively, before slightly declining towards the end of the 140-second interval. Fuel cell and controller exhibit moderate temperature rises, stabilizing at approximately 330 K and 320 K, respectively. DC/DC converter and rectifier experience a gradual increase, reaching about 310 K and 305 K. Battery maintains the lowest temperature, slightly increasing to just above 290 K.

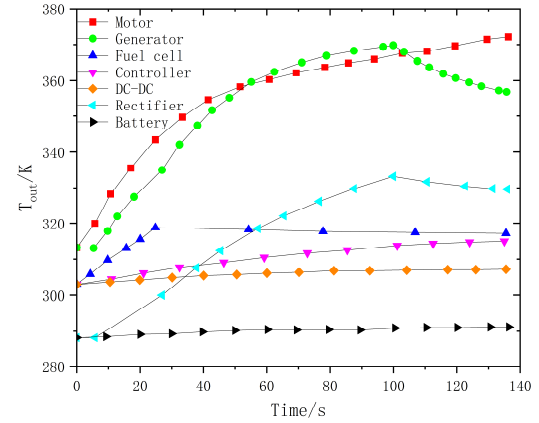


Fig. 15. Outlet temperatures for different electrical components in a DTCS architecture.

Table III presents the maximum inlet ( $T_{in,max}$ ) and outlet ( $T_{out,max}$ ) temperatures of various electrical components in both CTCS and DTCS architectures across all flight phases. Additionally, the table lists the maximum inlet temperature limits ( $T_{in,lim}$ ) for each electrical device, consistent with the data in Table II.

TABLE III. INLET, OUTLET AND LIMITED TEMPERATURES FOR DIFFERENT ELECTRICAL COMPONENTS IN CTCS AND DTCS ARCHITECTURE.

Components	$T_{in,max}$ /K (DTCS)	$T_{in,max}$ /K (CTCS)	$T_{in,lim}$ /K	$T_{out,max}$ /K (DTCS)	$T_{out,max}$ /K (CTCS)
Rectifier	289	303	343.15	333.1	330.5

Battery	289	311.7	293.15	291.1	313.6
DC/DC	303	303	333.15	307.5	310.5
Controller	303	345.5	343.15	315.3	349.4
FC	303	303.4	333.15	318.6	320.1
Motor	323.2	313.8	333.15	372.4	372.4
Generator	314.7	316.9	318.15	369.9	445.9

Rectifier and DC/DC converter show relatively stable and acceptable temperature performances in both systems, with their input temperatures staying well below their respective critical limits.

Battery and controller exhibit more significant temperature discrepancies, especially under CTCS. Battery in CTCS approaches its lower temperature limit closely, while the controller exceeds its upper temperature limit, indicating potential overheating issues.

Motor and Generator under both systems demonstrate concerning trends with output temperatures significantly exceeding the input temperatures, suggesting inefficiencies or potential risks in heat management that could impact the overall system performance and safety.

Comparing the simulation results of the two architectures, it can be observed that under the same parameter inputs, the temperature control effect of the CTCS is inferior to that of the DTCS architecture, with some components exceeding the temperature limits. To achieve better performance, it is necessary to increase the working fluid flow rate and other parameters, which may adversely affect the TCS weight, which further corroborates the advantages of the distributed architecture from a simulation perspective.

## REFERENCES

- [1] Chen W, Yang S, Dong S. Integrated Aircraft Thermal Management System Modelling and Simulated Analysis[J]. DEStech Transactions on Engineering and Technology Research, 2017(iceta).
- [2] Adler E J, Brelje B J, Martins J R R A. Thermal Management System Optimization for a Parallel Hybrid Aircraft Considering Mission Fuel Burn[J]. Aerospace, Multidisciplinary Digital Publishing Institute, 2022, 9(5): 243.
- [3] Affonso W, Tavares RenataT, Barbosa F R, et al. System architectures for thermal management of hybrid-electric aircraft - FutPrInt50[J]. IOP Conference Series: Materials Science and Engineering, 2022, 1226(1): 012062.
- [4] Stalcup E J, Heersema N. Thermal Requirements for Design and Analysis of Subsonic Single Aft Engine (SUSAN) Research Aircraft[A]. AIAA SCITECH 2023 Forum[C]. National Harbor, MD & Online: American Institute of Aeronautics and Astronautics, 2023
- [5] Maria C, David B, Alain S, et al. A review on the recent developments in thermal management systems for hybrid-electric aircraft [J]. Applied Thermal Engineering, 2023.
- [6] Coutinho M, Afonso F, Souza A, et al. A Study on Thermal Management Systems for Hybrid-Electric Aircraft[J]. Aerospace, 2023, 10(9): 745.
- [7] Chapman J W, Hasseeb H, Schnulo S. Thermal Management System Design for Electrified Aircraft Propulsion Concepts[A]. 2020 AIAA/IEEE Electric Aircraft Technologies Symposium (EATS)[C]. 2020: 1–23.
- [8] Chapman J W, Schnulo S L, Nitzsche M P. Development of a Thermal Management System for Electrified Aircraft[A]. AIAA Scitech 2020 Forum[C]. Orlando, FL: American Institute of Aeronautics and Astronautics, 2020.
- [9] Herber D R, Allison J T, Buettner R, et al. Architecture Generation and Performance Evaluation of Aircraft Thermal Management Systems Through Graph-based Techniques[A]. AIAA Scitech 2020 Forum[C]. Orlando, FL: American Institute of Aeronautics and Astronautics, 2020.
- [10] Kellermann H, Lüdemann M, Pohl M, et al. Design and Optimization of Ram Air-Based Thermal Management Systems for Hybrid-Electric Aircraft[J]. Aerospace, 2020, 8(1): 3.
- [11] Rheaume J M, Lents C E. Commercial Hybrid Electric Aircraft Thermal Management Sensitivity Studies[A]. AIAA Propulsion and Energy 2020 Forum[C]. VIRTUAL EVENT: American Institute of Aeronautics and Astronautics, 2020.
- [12] J. VAN MUIJDEN, J. AALBERS. Thermal Management Principal Analysis of Hybrid-Electric Aircraft with Turboelectric Propulsion Using Distributed Propulsors[A]. Proceedings of the 9th European Conference for Aerospace Sciences. Lille, France, 27 June - 1 July, 2022, 2022: 15 pages.
- [13] Mao Y-F, Li Y-Z, Wang J-X, et al. Cooling Ability/Capacity and Exergy Penalty Analysis of Each Heat Sink of Modern Supersonic Aircraft[J]. Entropy, 2019, 21(3): 223.
- [14] Glebocki M, Jain N, Malatesta W A, et al. Exergy-based Analysis and Optimization of Complex Aircraft Thermal Management Systems[J]. AIAA SCITECH 2022 Forum, 2022.
- [15] Schiltgen B T, Freeman J. Aeropropulsive Interaction and Thermal System Integration within the ECO-150: A Turboelectric Distributed Propulsion Airliner with Conventional Electric Machines[A]. 16th AIAA Aviation Technology, Integration, and Operations Conference[C]. Washington, D.C.: American Institute of Aeronautics and Astronautics, 2016.
- [16] Rheaume J M, Macdonald M, Lents C E. Commercial Hybrid Electric Aircraft Thermal Management System Design, Simulation, and Operation Improvements[A]. 2019 AIAA/IEEE Electric Aircraft Technologies Symposium (EATS)[C]. 2019: 1–23.
- [17] Shi M, Sanders M, Alahmad A, et al. Design and Analysis of the Thermal Management System of a Hybrid Turboelectric Regional Jet for the NASA ULI Program[A]. 2020 AIAA/IEEE Electric Aircraft Technologies Symposium (EATS)[C]. 2020: 1–24.